Non-Fickian Diffusion of Water in Polylactide

ARTICLE *in* INDUSTRIAL & ENGINEERING CHEMISTRY RESEARCH · DECEMBER 2012

Impact Factor: 2.59 · DOI: 10.1021/ie302342m

4 AUTHORS, INCLUDING:

Eric M. Davis
Clemson University
16 PUBLICATIONS **81** CITATIONS
SEE PROFILE

Matteo Minelli
University of Bologna
66 PUBLICATIONS **315** CITATIONS
SEE PROFILE

Marco Giacinti Baschetti
University of Bologna
73 PUBLICATIONS **652** CITATIONS
SEE PROFILE

I&EC research
Industrial & Engineering Chemistry Research

Article

pubs.acs.org/IECR

Non-Fickian Diffusion of Water in Polylactide

Eric M. Davis,[†] Matteo Minelli,[‡] Marco Giacinti Baschetti,[‡] and Yossef A. Elabd*,[†]

[†]Department of Chemical and Biological Engineering, Drexel University, Philadelphia, Pennsylvania 19104, United States
[‡]Dipartimento di Ingegneria Chimica Mineraria e delle Tecnologie Ambientali (DICMA), Università di Bologna, 40131 Bologna, Italy

Supporting Information

ABSTRACT: The diffusion of water in polylactide (PLA) was measured at various external water vapor activities (0−0.85) and temperatures (25, 35, 45 °C) using three separate experimental techniques: quartz spring microbalance (QSM), quartz crystal microbalance (QCM), and time-resolved Fourier transform infrared-attenuated total reflectance (FTIR-ATR) spectroscopy. Non-Fickian sorption kinetic behavior was observed with all the experimental techniques used over the observed experimental time scales, which was a result of the nonequilibrium state of the glassy polymer. Two phenomena were observed over two distinct time periods (two-stage sorption kinetics), where early time data revealed diffusion driven by a water concentration gradient and later time data revealed diffusion driven by slow polymer relaxation or swelling due to additional water ingress over time. Diffusion coefficients and relaxation time constants were determined by regressing the early time data to a Fickian model and the data over the entire observed experimental time scale to a diffusion-relaxation model, respectively. Diffusion coefficients increased with temperature, were constant with activity and concentration of water in the polymer, and were similar among all three experimental techniques. The high Deborah numbers (relaxation time/diffusion time) determined from the diffusion-relaxation model confirm the observed two-stage non-Fickian behavior.

INTRODUCTION

Biodegradable polymers, such as polylactide (PLA), are attractive because they can be synthesized from renewable sources and readily degrade over time into benign naturally occurring small molecules.[1] Currently, PLA is being considered as a future replacement to widely used commodity plastics, which are synthesized from nonrenewable sources, for a variety of different applications, such as food packaging and medical implants.[1−4] Therefore, a detailed understanding of water transport in PLA is of great interest; however, there are only a few published reports on the transport of water in PLA.[4−9] Mainly, these investigations have focused on the effect of polymer crystallinity on water sorption with conflicting results.[5,6,9] Other studies report slight variations in water diffusivity and solubility in amorphous PLA samples of varying D and L isomer content.[4−5] However, all of these reports assume sorption kinetics or diffusion of water in PLA to be Fickian.

Recent results by Davis and co-workers[8] on the diffusion of liquid water in PLA, however, show non-Fickian diffusion behavior. This is an expected result for the diffusion of small molecules in a glassy polymer (at an experimental temperature below the glass transition temperature of the polymer), where others have observed non-Fickian or diffusion-relaxation phenomena for the diffusion of organics in glassy polymers.[10−12] In this early work, it was suggested that two phenomena are observed on the same experimental time scale, one due to diffusion driven by the penetrant concentration gradient, while the other is due to additional slow ingress of the penetrant driven by stress-induced polymer relaxation or swelling owing to the nonequilibrium state of the polymer, that is, the polymer relaxes or swells on a similar time scale as the experimental time scale. Both of these phenomena are clearly shown in the work by Davis et al.[8] on the diffusion of liquid water in PLA homopolymers and graft copolymers using time-resolved Fourier transform infrared, attenuated total reflectance (FTIR-ATR) spectroscopy. In their work, they were able to simultaneously quantify both water diffusion and polymer relaxation from different mid-infrared vibrational bands and subsequently accurately regressed both sets of data to a diffusion-relaxation model to determine both the water diffusion coefficient and the polymer relaxation time constant with a minimal set of fitting parameters. In addition, Davis and co-workers[13] have recently measured the nonequilibrium sorption of water vapor in PLA using two separate gravimetric techniques: quartz spring microbalance (QSM) and quartz crystal microbalance (QCM), and accurately predicted the experimental water sorption data at various vapor activities and temperatures with a nonequilibrium lattice fluid (NELF) model. The sorption kinetics for water vapor transport in PLA was also non-Fickian[13] similar to the liquid water diffusion results previously reported.[8] However, the analysis of non-Fickian water vapor diffusion in PLA has yet to be investigated in detail.

In this study, the diffusion of water vapor in amorphous PLA was investigated with three separate experimental techniques: QSM, QCM, and time-resolved FTIR-ATR spectroscopy at various vapor activities, different experimental temperatures (25, 35, 45 °C; all below the glass transition temperature of PLA), and different film thicknesses. Non-Fickian behavior was observed with all three techniques, where two phenomena were observed to occur over two distinct time periods (two-stage behavior) in the

Special Issue: Giulio Sarti Festschrift

Received: August 31, 2012
Revised: November 28, 2012
Accepted: November 29, 2012
Published: November 29, 2012

dx.doi.org/10.1021/ie302342m | Ind. Eng. Chem. Res. 2013, 52, 8664−8673

same experimental time scale; diffusion driven by a water concentration gradient for the first stage and diffusion driven by a slower (relative to the first stage) polymer relaxation for the second stage. The sorption kinetics data were regressed to a diffusion-relaxation model to determine the water diffusion coefficients and relaxation time constants.

EXPERIMENTAL SECTION

Materials. Polylactide (PLA) (M_w = 140 600 g/mol, PDI = 2.27, T_g = 57 °C) was purchased from Nature Works LLC in pellet form (PLA 4060D, a racemic mixture of D/L isomers); chemical structure shown in Figure 1. The molecular weight,

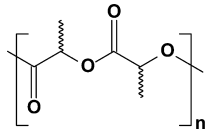

Figure 1. Chemical structure of polylactide (PLA).

PDI, and T_g of PLA were determined using gel permeation chromatography (GPC) and differential scanning calorimetry (DSC) and published previously.[13] The DSC data confirmed that the PLA used in this study was completely amorphous. Chloroform (99.8% purity; ACS reagent) was purchased from Aldrich. Double distilled deionized water (conductivity = 0.01 μS/cm) was used for all experiments.

Film Preparation. PLA/chloroform solutions were prepared by dissolving PLA pellets in chloroform at 5% w/w and mixing for 24 h to ensure a clear, homogeneous solution. PLA film fabrication consisted of solution casting the PLA/chloroform solution onto a Teflon Petri dish to produce free-standing films for QSM experiments or solution casting onto the ATR crystal surface for time-resolved FTIR-ATR spectroscopy experiments. For both QSM and ATR experiments, the polymer solution was dried in ambient conditions for 24 h after deposition. This was followed by annealing the film at 70 °C under vacuum for 3 h. For QCM experiments, PLA films were spun-coat unto a gold QCM crystal (15 s at 900 rpm, followed by 15 s at 1500 rpm). Before the annealing process, the stability of the PLA-coated QCM crystals was evaluated (i.e., the frequency of the coated crystal was monitored over time). If the baseline frequency drift of the coated crystal was too large, the coated crystal was then placed back in the spin coater and exposed to a drop of pure chloroform at 1000 rpm. This was then followed by the aforementioned annealing protocol. After film fabrication, all PLA films were immediately stored in a desiccator prior to all experiments. Immediately following each experiment, the thickness of the PLA films for QSM and ATR experiments was measured using a digital micrometer (Mitutoyo) with a 1 μm accuracy. Each film thickness was an average of at least three individual measurements at different positions along the length of the film. Average film thicknesses for the QSM, QCM, and ATR experiments were ca. 80−150 μm, 7 μm, and 90 μm. The thickness for the QCM experiments was estimated from the measured polymer mass, the electrode area, and the polymer density (1.24 g/cm^3).

Quartz Spring Microbalance (QSM). A PLA film (ca. 50 mg), along with metal reference (ca. 20 mg), was placed at the end of a vertical quartz spring (purchased from DeerSlayer Springs; 100 mg max load with 500 mm max extension; spring constant, k_{spring} = 0.98 g/s^2), which was housed inside a temperature-controlled glass column. The glass column, along with a temperature-controlled reservoir,[13] was completely evacuated of moisture and air *via* vacuum for at least 2 h. After the system was completely evacuated, the valve connecting the glass column housing the quartz spring and sample to the rest of the experimental setup was closed (leak rate less than 0.2 mmHg/day). The reservoir containing deionized water was subjected to a number of freeze−thaw vacuum cycles in order to remove all dissolved gases from the liquid. Pure water vapor was then charged into the temperature-controlled reservoir at specific partial pressures, where it was allowed to equilibrate with the temperature of the jacket until steady-state was reached (i.e., the pressure transducer reading was constant). Once steady-state was reached, the valve separating the reservoir from the glass column was fully opened, exposing the PLA film in the glass column to a specified partial pressure of water. The change in the extension of the spring due to water sorbing into the polymer was measured as a function of time with a high-speed charge coupled device (CCD) camera (DVT SmartImage Sensor-Series 600 model 630). The mass of water sorbed in PLA was calculated from this spring extension data with the use of the spring constant and a force balance, that is, $F = mg = kx$. The water diffusion coefficient can be obtained from regressing the experimental data (mass versus time) to the solution of Fick's second law. This solution is obtained by solving the one-dimensional continuity equation for a film in rectangular coordinates with the appropriate initial and boundary conditions for this experiment:

$$\frac{\partial C}{\partial t} = D\frac{\partial^2 C}{\partial z^2} \tag{1}$$

In eq 1, C is the concentration of the diffusant (in this case water), D is the effective concentration-averaged diffusion coefficient of water in the polymer, and t and z are time and space coordinates, respectively. For the QSM case, where the sorption of water in the polymer film of thickness $2L$ ($-L < z < L$) occurs from both sides of the film and $z = 0$ corresponds to the center of the film (symmetric condition), the appropriate initial and boundary conditions for this experiment are

$$C(t = 0, z); \quad \frac{\partial C}{\partial t}(t, z = 0) = 0; \quad C(t, z = L) = C_{eq} \tag{2}$$

In eq 2, C_{eq} is the final equilibrium concentration of water in the polymer (i.e., constant surface concentration of water in the polymer at the water-polymer interface). An analytical solution to eq 1 with these initial and boundary conditions (eq 2) is given as[14]

$$\frac{C(t, z)}{C_{eq}} = 1 - \frac{4}{\pi}\sum_{n=0}^{\infty}\frac{(-1)^n}{2n+1}\exp\left[\frac{-D(2n+1)^2\pi^2 t}{4L^2}\right] \times \cos\left[\frac{(2n+1)\pi z}{2L}\right] \tag{3}$$

For the case of the QSM gravimetric experiment, the following equation in terms of mass can be derived from eq 3:[14]

$$\frac{M(t)}{M_{eq}} = 1 - \sum_{n=0}^{\infty}\frac{8}{(2n+1)^2\pi^2}\exp\left[\frac{-D(2n+1)^2\pi^2 t}{4L^2}\right] \tag{4}$$

where $M(t)$ and M_{eq} denotes the total amount of water that diffuses into the polymer film at time t, and at equilibrium, respectively, and D is the diffusion coefficient of water. Therefore, the QSM gravimetric data can be regressed to eq 4 to determine D, which is

dx.doi.org/10.1021/ie302342m | Ind. Eng. Chem. Res. 2013, 52, 8664−8673

the only adjustable parameter in this model. More details about this apparatus and procedures can be found elsewhere.[13]

Quartz Crystal Microbalance (QCM). The entire QCM apparatus (purchased from Elbatech, Italy), including sample chamber and water reservoir, was enclosed and sealed in a metal tank and completely submerged in a temperature-controlled bath, where water vapor at specific partial pressures was charged into the sample chamber. The QCM measures the frequency shift of a 9 MHz AT cut quartz crystal (Kyushu Dentsu Co., Ltd., Japan). Raw frequency values were converted to actual mass uptake in the PLA film through the use of the Sauerbrey equation:[15]

$$\Delta f = \left[\frac{-2{f_0}^2}{A\sqrt{\rho_Q G_Q}}\right]\Delta m \tag{5}$$

where Δf is the change in frequency to due to the addition of sorbed mass, f_o is the resonance frequency of the bare oscillator, A is the surface area of the coated crystal, and ρ_Q and G_Q are the density and shear modulus of the quartz, respectively. Once the change in mass is obtained from the change in frequency data with the use of eq 5, then a diffusivity can be obtained by regressing these data to eq 4, similar to the analysis of the QSM data. Note that the film thickness in QCM differs from QSM, where water can only sorb into one side of the film since the other side is adhered to the quartz crystal ($z = 0$), that is, the coordinates were chosen so that $z = 0$ is the polymer-crystal interface and $z = L$ is the water−polymer interface. Therefore the film thickness in QCM is L instead of $2L$ as was the case for QSM. More details regarding the experimental apparatus and experimental procedures can be found elsewhere.[16]

Time-Resolved FTIR-ATR Spectroscopy. Water sorption was also measured with time-resolved infrared spectroscopy using an FTIR spectrometer (Nicolet 6700 Series; Thermo Electron) equipped with a horizontal, temperature-controlled ATR cell (Specac Inc.). The PLA films were deposited on a multiple reflection, trapezoidal zinc selenide ATR crystal (Specac Inc.) with 45° beveled faces. All spectra were collected using a liquid nitrogen-cooled mercury−cadmium−telluride (MCT) detector with 32 scans per spectrum at a resolution of 2 cm^{-1}, where a spectrum was collected every 15 s. The temperature of all transport experiments was controlled by a temperature jacket (circulated water bath) on the ATR flow through cell. The ATR flow through cell was connected directly to the vapor sorption apparatus.

Before each transport experiment, a background spectrum of the bare ATR crystal was collected and all subsequent collected spectra were subtracted from this spectrum. Then, a PLA coated ATR crystal was mounted into the ATR flow through cell with a Kalrez gasket and the cell was sealed. The reservoir in the vapor sorption apparatus contained pure liquid water and was subjected to multiple freeze−thaw−vacuum cycles in order to ensure complete removal of any dissolved gases from the water.

To begin each transport experiment, the vapor sorption/ATR combined system was evacuated for at least 2 h prior to beginning each experiment (i.e., pressure transducer reached constant value). Then pure water vapor was charged into the vapor sorption system at a specific partial pressure and allowed to equilibrate (i.e., the pressure transducer reading was constant). Once this equilibrium was reached, the valve separating the ATR cell from the rest of the system was opened, allowing pure water vapor to enter the ATR cell in the space ($V = 550\ \mu L$) above the polymer film (the side opposite the polymer−crystal interface). This was followed by the collection of time-resolved infrared spectra.

To determine the diffusivity of water in the polymer using FTIR-ATR spectroscopy, the concentration can be related to the ATR experimental absorbance through the use of the differential form of the Beer−Lambert law (eq 6), where an evanescent wave propagates into the polymer due to total internal reflection physics at the polymer-crystal interface.[17]

$$A = \int_0^L \varepsilon^* C \exp\left(\frac{-2z}{d_p}\right) dz \tag{6}$$

In eq 6, A is the ATR absorbance value, ε^* is the molar extinction coefficient (which can be considered constant under the assumption of weak IR absorbance, which is the case in this study), and d_p is the depth of penetration for the IR radiation in the polymer:

$$d_p = \frac{\lambda}{2\pi n_1\sqrt{\sin^2\theta - (n_2/n_1)^2}} \tag{7}$$

n_1 and n_2 are the refractive indices of the ATR crystal and polymer, respectively, θ is the angle of incidence, and λ is the wavelength of absorbed light. The depth of penetration is essentially the sampling distance into the polymer, which is when the evanescent wave has decayed to approximately $^1/_3$ of its maximum intensity (~1 μm for these experiments). Substituting eq 3 into eq 6 and integrating results in the following expression gives[19]

$$\frac{A(t)}{A_{eq}} = 1 - \frac{(8/d_p)}{\pi[1 - \exp(-2L/d_p)]}\sum_{n=0}^{\infty}\left(\frac{\exp\left[\frac{-D(2n+1)^2\pi^2 t}{4L^2}\right]\left[\frac{(2n+1)\pi}{2L}\exp(-2L/d_p) + (-1)^n(2/d_p)\right]}{(2n+1)\left((2/d_p)^2 + \left(\frac{(2n+1)\pi}{2L}\right)^2\right)}\right) \tag{8}$$

where $A(t)$ and A_{eq} are the ATR absorbance at time t and at equilibrium (i.e., long times), respectively.

When $L/d_p > 10$, the concentration profile near the polymer/crystal interface is constant resulting in a location-specific solution (thick-film approximation).[18]

$$\frac{A(t)}{A_{eq}} = 1 - \frac{4}{\pi}\sum_{n=0}^{\infty}\frac{(-1)^n}{2n+1}\exp\left[\frac{-D(2n+1)^2\pi^2 t}{4L^2}\right] \tag{9}$$

In other words, the concentration profile or gradient in the measured region (~1 μm in the polymer film near the polymer/crystal interface) is constant when the polymer film thickness is much larger than the sampling depth, resulting in a location-specific measurement. Therefore, water is imposed on one side of the film and measured on the other side as a function of time. Equation 9 can therefore be regressed to the experimental time-resolved ATR absorbance of water vapor in PLA to determine an effective diffusion coefficient, where this variable is the only adjustable parameter in the model. Similar to the QCM experiment, water can only sorb into one side of the film since the other side is adhered to the ATR crystal ($z = 0$), that is, the coordinates were chosen so that $z = 0$ is the polymer−crystal

dx.doi.org/10.1021/ie302342m | Ind. Eng. Chem. Res. 2013, 52, 8664−8673

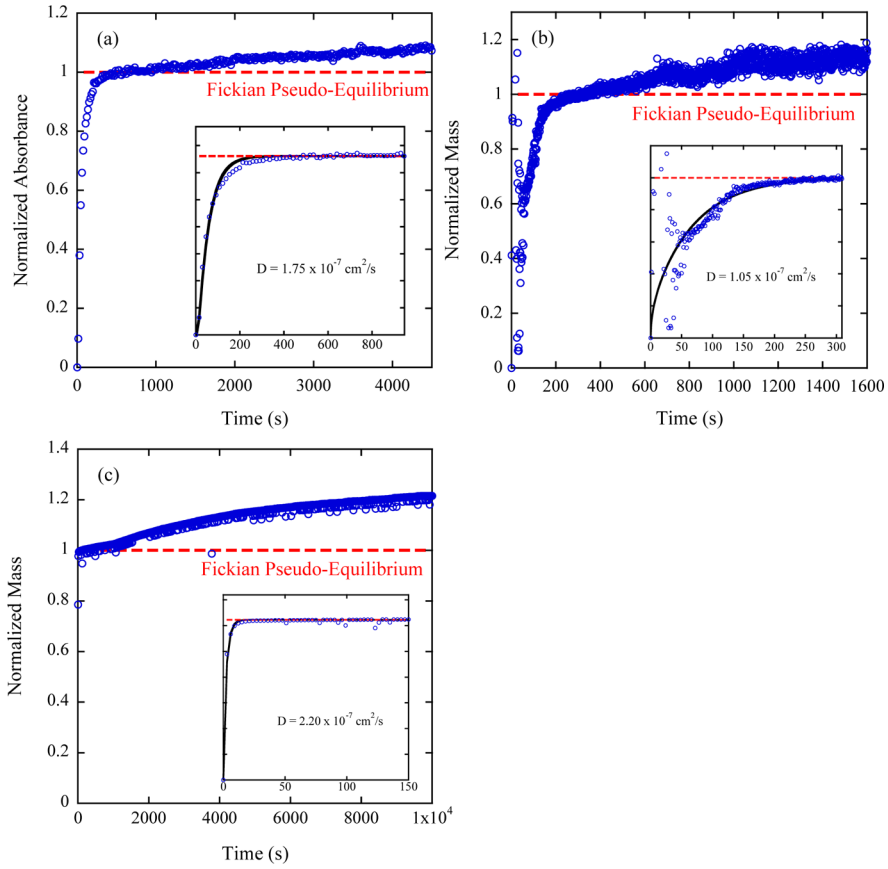

Figure 2. Water sorption kinetics in PLA at 35 °C measured with (a) time-resolved FTIR-ATR spectroscopy, (b) QSM, and (c) QCM in response to an external differential change in water vapor activity of 0.54 to 0.75, 0.53 to 0.65, and 0.25 to 0.36, respectively. The insets correspond to magnified view of the early time data, where the solid lines correspond to a regression to the solution to Fick's Second Law (eqs 9, 4, and 4 for panels a, b, and c, respectively), where the diffusion coefficient, D, was the only adjustable parameter. The dashed lines correspond to pseudoequilibrium values.

interface and $z = L$ is the water−polymer interface. Therefore the film thickness, L, in ATR is similar to QCM and differs from QSM (film thickness = $2L$). More details regarding the apparatus and experimental procedures can be found elsewhere.[19]

RESULTS AND DISCUSSION

Non-Fickian Diffusion. The diffusivity of water in PLA was measured using three experimental techniques: time-resolved FTIR-ATR spectroscopy, QSM, and QCM, as a function of external water vapor activity and temperature. All experiments in this study were conducted at 25, 35, and 45 °C, all below the glass transition temperature of PLA. Figure 2 shows the water sorption kinetics in PLA at 35 °C after a differential change of the external water vapor activity for all three experimental techniques. Data from all three techniques exhibit similar anomalous or non-Fickian diffusion.

Other investigators have observed similar behavior in appearance for the diffusion of small molecule organics in glassy polymers.[10−12] This behavior was attributed to the nonequilibrium state of the glassy polymer, where initially diffusion is driven by the concentration gradient of the diffusant and at longer times it is driven by polymer relaxation or swelling, which occurs in response to the stress imposed by the diffusant.[10,11] In other words, this anomalous behavior is a product of the nonequilibrium nature of the polymer. Therefore, if the experiment were conducted at a temperature above the glass transition temperature of the polymer (rubbery polymer), the polymer is in an equilibrium state and would respond instantaneously (elastic) to the stress imposed by water ingress and therefore this relaxation phenomena would not be observed over this experimental time scale. However, at experimental temperatures below the glass transition temperature of the polymer (glassy polymer), the polymer is in a nonequilibrium state and polymer relaxation occurs over a much slower time scale (viscoelastic) and can be captured over observable experimental time scales.

For the case of water diffusion in PLA, as shown in Figure 2, these two phenomena are observed and occur over two distinct time periods (two-stage sorption kinetics) over the entire experimental time. The insets in Figure 2 illustrate the first period or stage, where Fickian-like or pseudo-Fickian behavior was observed in all three experiments. Here, one can regress these data in this initial short time scale to the solution of Fick's Second Law (eqs 9, 4, and 4 for Figures 2a, 2b, and 2c, respectively), with the remarkable feature that for all three experimental techniques the same Fickian diffusivity was obtained (ca. 1×10^{-7} cm^2/s) within experimental errors. However, at longer experimental times, the glassy polymer relaxes due to its nonequilibrium state and gradually allows more water into the polymer over the observed time scale. In Figure 2, the data were normalized to the mass or absorbance at the pseudoequilibrium time point for simplicity even though this is not the mass or absorbance at a final equilibrium time point, which was never observed in these experimental time scales.

It is important to note that if the experimental times were shorter, similar to the time scale of the insets in Figure 2, the diffusion of water in PLA would appear Fickian. Therefore, the

dx.doi.org/10.1021/ie302342m | Ind. Eng. Chem. Res. 2013, 52, 8664−8673

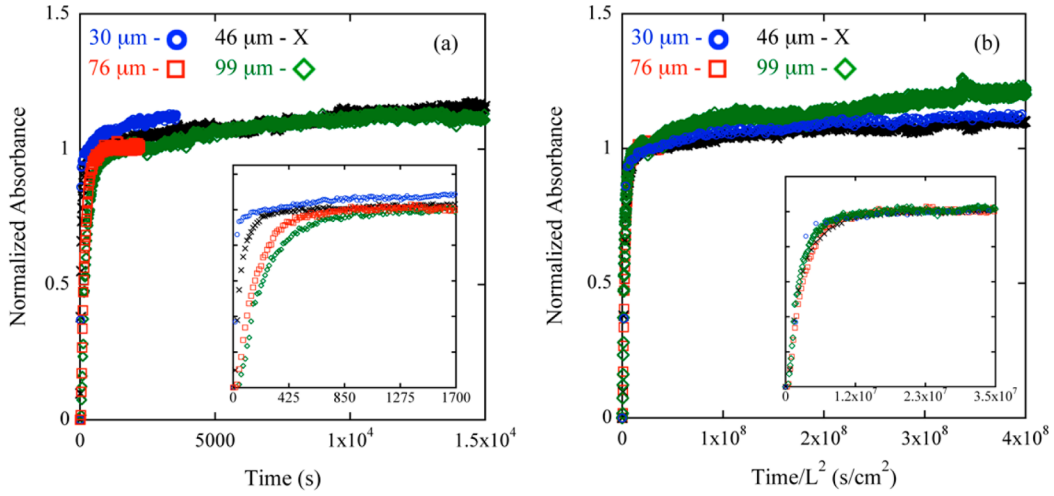

Figure 3. Time-resolved FTIR-ATR spectroscopy data: normalized, integrated absorbance of the water O−H infrared stretching band in PLA at 35 °C for four different PLA film thicknesses of 30, 46, 76, and 99 μm (a) plotted versus time and (b) plotted versus normalized time (i.e., time divided by film thickness squared). Insets correspond to magnified view of the early time data.

time scale of the experiment (in relation to the thickness of the polymer) is an important feature as it relates to the measurement of diffusivity and solubility. On the basis of the full data set shown in Figure 2, one could report an infinite number of sorption values after the pseudo-Fickian regime depending on the length of the experiment. In previous work,[13] we report solubility of water in PLA at the pseudo-Fickian plateau observed in the insets in Figure 2 as a consistent reference for comparison between different experimental techniques. The pseudo-Fickian or pseudo-equilibrium solubility measured in this fashion was equivalent when the QSM and QCM data were compared at all vapor activities.[13] An analysis of the pseudo-equilibrium solubility of water in PLA has been reported previously,[13] therefore the focus of this study is to examine the sorption kinetics or diffusion.

When examining diffusion, it is worth recalling that the experimental time and polymer film thickness are inherently coupled. In this study, the PLA film thicknesses were different between the FTIR-ATR (ca. 90 μm), QSM (ca. 80−150 μm), and QCM (ca. 7 μm) experiments, which results in a shorter time to reach the pseudo-Fickian plateau in the QCM experiment (ca. 10 s) compared to the ATR (ca. 800 s) and QSM (ca. 200−600 s) experiments. It is also worth recalling here that different experimental apparatus lead to different diffusional geometries, and hence different diffusional path lengths. For free-standing films, the diffusional geometry is such that symmetry exists in the center of the film (film thickness of $2L$), causing the diffusional path for these experiments to be half that of the total thickness of the film. In contrast, films cast directly on a substrate do not contain this symmetry, and therefore the entire thickness of the film must be considered (film thickness of L). If experiments were conducted with shorter experimental times or thicker films, only Fickian behavior would be observed. Therefore, great care must be taken for each experiment to extend the experimental time for the film thickness used to appropriately observe the non-Fickian diffusion−relaxation phenomena.

To examine this concept further, time-resolved FTIR-ATR spectroscopy measurements of water diffusion in PLA were performed on films of different thicknesses. Figure 3 shows these data at 35 °C on PLA films of 30, 46, 76, and 99 μm in thickness. The early time data, shown in the inset in Figure 3a, highlights that the pseudo-Fickian plateau can be achieved at a much shorter time in the 30 μm thick film (ca. 90 s) compared to the 99 μm thick film (ca. 1000 s). Additionally, at longer experimental times, the second stage (water diffusion due to polymer relaxation) is more easily observable in the thinner film compared to the thicker film, evidenced by a steeper slope in the second phase of the 30 μm thick film data over this time scale. Collecting data over even longer experimental times will be required to more clearly observe the effect of polymer relaxation on water diffusion in thicker films.

To further illustrate this film thickness−time coupling, Figure 3b shows a plot of the data in Figure 3a plotted versus a normalized time scale or experimental time divided by the square of the polymer film thickness for each PLA film. Interestingly, the water diffusion data collapse onto a universal curve at early experimental times and vary over longer experimental times. This further confirms the two-stage diffusion-relaxation phenomena, where Fickian diffusion is expected to scale with the square of the film thickness (L^2) and relaxation should be thickness independent.[10] Additionally, this normalization provides a universal time scale, where for all film thicknesses, the pseudo-Fickian plateau is reached in ca. 1×10^7 s/cm^2.

It is also worth noting that if diffusion experiments were conducted above the T_g (57 °C) of PLA, then one should observe purely Fickian kinetics at all thicknesses and experimental time scales, because the polymer would be in an equilibrium state. However, performing experiments at higher temperatures in PLA specifically will also result in well-known moisture-induced chemical degradation. Our attempts to measure water diffusion in PLA at 65 °C resulted in noticeable chemical degradation due to polymer hydrolysis, which was observed both spectroscopically and in a loss of mass over time at high water vapor activities. Therefore, purely Fickian kinetics alone was not observed at higher temperatures due to its combined effect with chemical degradation.

Pseudo-Fickian Diffusion. To quantify the diffusivity of water in PLA, the early time data (first stage) or pseudo-Fickian portion of the sorption kinetics curves were evaluated for all three experimental techniques over the entire vapor activity range. Figure 4 shows water diffusivity measured by time-resolved FTIR-ATR spectroscopy at 35 °C. Specifically, multiple sorption curves are shown in response to multiple differential step changes in external water vapor activity ranging from 0.1 to 0.2 for each step over a broader range of 0 to 0.85. On shorter experimental time scales, all sorption curves in Figure 4 appear Fickian-like,

dx.doi.org/10.1021/ie302342m | Ind. Eng. Chem. Res. 2013, 52, 8664−8673

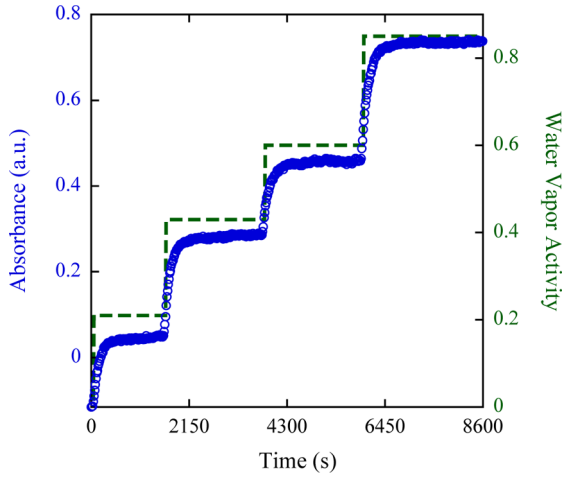

Figure 4. Time-resolved FTIR-ATR spectroscopy data at 35 °C: multiple water sorption kinetic curves (water O−H infrared absorbance band at 3660 cm^{-1}) in PLA in response to multiple differential external water vapor activities over a broad range of 0 to 0.85 for entire sorption experiment.

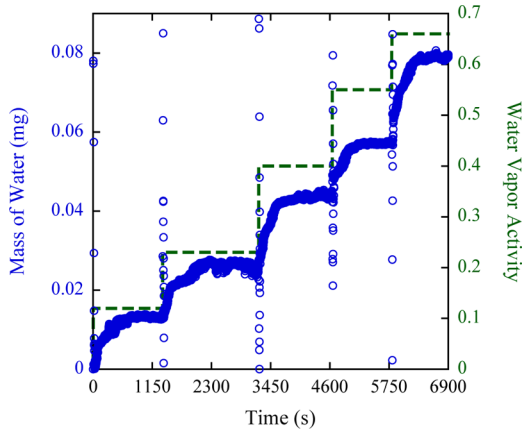

Figure 6. QSM data: multiple water sorption kinetic curves in PLA at 35 °C in response to multiple differential external water vapor activities over a broad range of 0 to 0.66 for entire sorption experiment.

where the normalized time scale for each step was ca. 1×10^7 s/cm^2 (or ca. 600 s for ca. 80 μm thick film).

For each pseudo-Fickian differential sorption step, diffusion coefficients were calculated from regressing the experimental data to the solution to Fick's Second Law (eq 9). An example of one regression is shown in Figure 5a for a single water sorption step in response to a water activity step change from 0.43 to 0.60, where a water diffusion coefficient of 1.80×10^{-7} cm^2/s was determined and an excellent agreement between data and model was obtained. This analysis was conducted on all sorption curves for multiple experiments at different temperatures. Figure 5b shows all of the diffusion coefficients calculated at 25, 35, and 45 °C over the entire water vapor activity range explored, where the values increase slightly with increasing temperature, but do not noticeably vary with activity. The latter trend may be the result of the low absolute solubility of water in PLA over the entire water vapor activity range.[13]

Figure 6 shows water diffusivity measured with QSM at 35 °C. Multiple sorption curves are shown in response to multiple differential step changes in external water vapor activity ranging from 0.1 to 0.2 for each step over a broader range of 0 to 0.66. Similar to the FTIR-ATR data, all sorption curves appear Fickian-like at these shorter experimental time scales, where the normalized time scale for each step was again ca. 1×10^7 s/cm^2 (or ca. 600 s for ca. 150 μm thick film).

Diffusion coefficients were calculated by regressing the experimental pseudo-Fickian sorption curves to the solution of Fick's Second Law (eq 4). An example of one of these regressions for a single differential sorption step (water activity change from 0.60 to 0.73) is shown in Figure 7a, where a water diffusion coefficient of 1.05×10^{-7} cm^2/s was calculated. This diffusion coefficient is similar to the value obtained with FTIR-ATR spectroscopy. This analysis was conducted on all sorption curves for multiple experiments at different temperatures. Figure 7b shows all of the diffusion coefficients calculated at 25, 35, and 45 °C over the entire water vapor activity range explored, where the values increase slightly with increasing temperature, but do not noticeably vary with activity; similar to what was observed with FTIR-ATR spectroscopy experiments.

The average diffusion coefficients calculated at 25, 35, and 45 °C were 8.52×10^{-8}, 1.17×10^{-7}, and 2.32×10^{-7} cm^2/s, respectively. The variation in diffusivity over the entire activity range at a given temperature was higher than what was observed with FTIR-ATR spectroscopy. This larger variation of the calculated

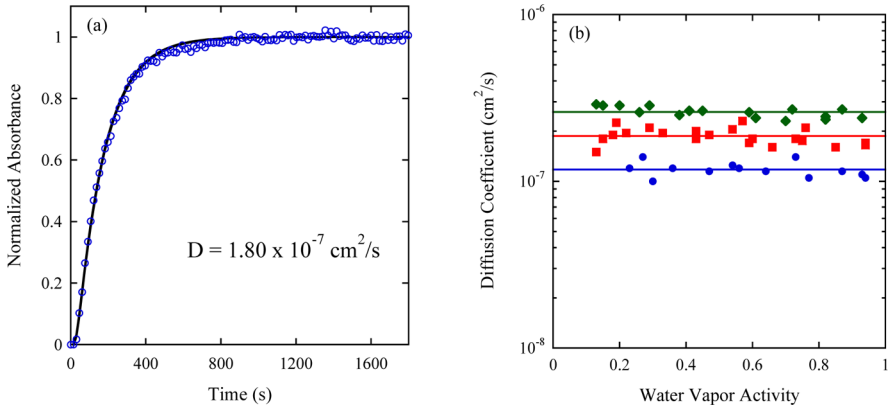

Figure 5. Time-resolved FTIR-ATR spectroscopy data: (a) water sorption kinetics (water O−H absorbance) in PLA at 35 °C in response to an external differential water vapor activity step change of 0.43 to 0.60. The solid black line represents a regression of the experimental data (open blue circles) to the solution to Fick's Second Law (eq 9), where the diffusion coefficient, D, was the only adjustable parameter. (b) Water diffusion coefficients in PLA over a wide range of water activities at 25 (blue circles), 35 (red squares), and 45 °C (green diamonds).

dx.doi.org/10.1021/ie302342m | Ind. Eng. Chem. Res. 2013, 52, 8664−8673

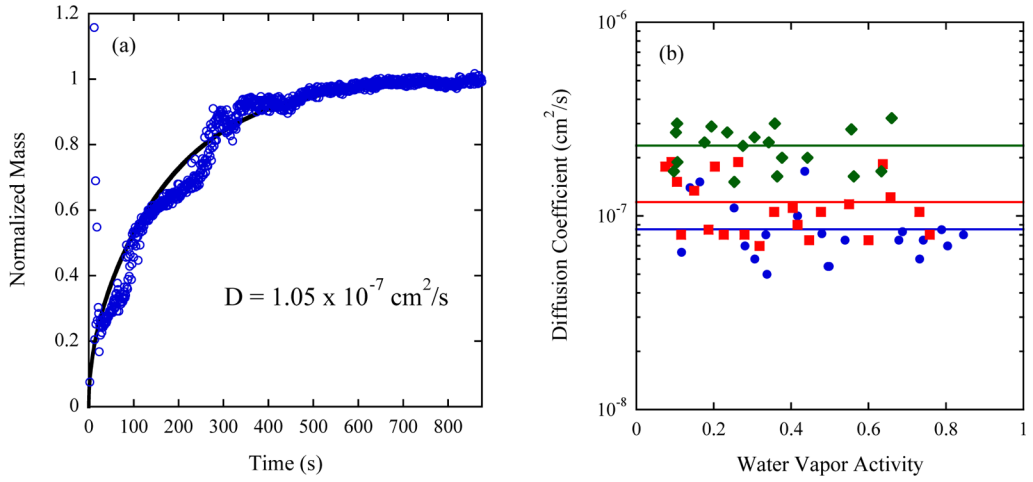

Figure 7. QSM data: (a) water sorption kinetics in PLA at 35 °C in response to an external differential water vapor activity step change of 0.60 to 0.73. The solid black line represents a regression of the experimental data (open blue circles) to the solution to Fick's Second Law (eq 4), where the diffusion coefficient, *D*, was the only adjustable parameter. (b) Water diffusion coefficients in PLA over a wide range of water activities at 25 (blue circles), 35 (red squares), and 45 °C (green diamonds).

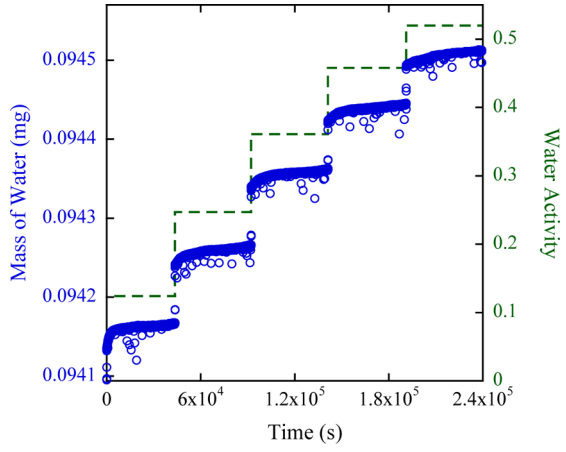

Figure 8. QCM data: multiple water sorption curves in PLA at 35 °C in response to multiple differential external water vapor activities over a broad range of 0−0.52 for the entire sorption experiment.

water diffusion coefficient may be attributed to the variation in experimental data during the initial uptake portion of kinetic curve due to the buoyancy forces of the spring. When water vapor is introduced into the evacuated sample chamber, the spring and sample oscillate in a decaying, periodic fashion. Depending on the thickness and weight of the sample, this oscillation in the water sorption kinetic data can contribute to a significant portion of the initial uptake curve, resulting in variation in the regressed diffusion coefficients obtained for water vapor in PLA.

The diffusivity of water was also examined with QCM at 35 °C. Multiple sorption curves are shown in Figure 8 in response to multiple differential step changes in external water vapor activity of ca. 0.1 for each step over a broader range of 0−0.52. Similar to the FTIR-ATR and QSM data, all sorption curves appear Fickian-like at shorter time scales, where the normalized time scale for each step was again ca. 1×10^7 s/cm^2 (or ca. 10 s for ca. 7 μm thick film).

It is interesting to note that in Figure 8 each differential sorption step was extended to approximately one day (ca. 20 h) in order to observe a significant portion of the polymer relaxation phenomena. From the early time data, diffusion coefficients were calculated by regressing the experimental pseudo-Fickian sorption curves to the solution of Fick's Second Law (eq 4). An example of one of these regressions for a single differential sorption step (water activity change from 0.25 to 0.36) is shown in Figure 9a, where a water diffusion coefficient of 2.20×10^{-7} cm^2/s was determined.

From Figure 9a, it is clear that the pseudoequilibrium state is reached in a time scale of seconds at the film thicknesses required for stable QCM analysis (ca. 7 μm). These rapid sorption kinetics introduce significant error when an attempt is made to determine an accurate diffusion coefficient, where only three or four data points are measured before reaching the pseudo-Fickian. This error is highlighted in Figure 9b, where the variation in the regressed diffusion coefficient over the entire activity range explored is higher than the results from ATR (Figure 5b) and QSM (Figure 7b). It is clear from Figure 9b that there is large variation in the calculated diffusion coefficient obtained QCM (ca. 45%). Overall, the regressed diffusion coefficient for FTIR-ATR data resulted in the lowest variation compared to the QSM and QCM experiments, where spring buoyancy and lack of early time data, respectively, result in higher errors. However, the diffusion coefficient calculated using each of the three experimental techniques are similar and are in a similar range as those reported in the literature.[1,5] The regressed Fickian diffusion coefficients for all experiments using all three experimental techniques are summarized in Supporting Information, Tables S1, S2, S3.

Diffusion-Relaxation Phenomena. To describe the transport mechanisms of water in PLA in more detail over the entire experimental time scale, the relaxation of the polymer in the presence of water vapor was examined. In a previous work by Davis et al.[8] on the diffusion of liquid water in PLA with the use of time-resolved FTIR-ATR spectroscopy, the CH_3 stretching absorbance band associated with the polymer was quantified as a function of time as a measure of polymer dilation and these data were regressed to a viscoelastic model to determine the polymer relaxation time constant. The non-Fickian water diffusion data (O−H stretching absorbance band) were then regressed to a diffusion-relaxation model to determine the diffusion coefficient using the polymer relaxation time constant from the polymer absorbance data as a fixed parameter. Similar to this previous work,[8] the mid-infrared spectra of the chemical bonds associated with the polymer during time-resolved FTIR-ATR spectroscopy

dx.doi.org/10.1021/ie302342m | *Ind. Eng. Chem. Res.* 2013, 52, 8664−8673

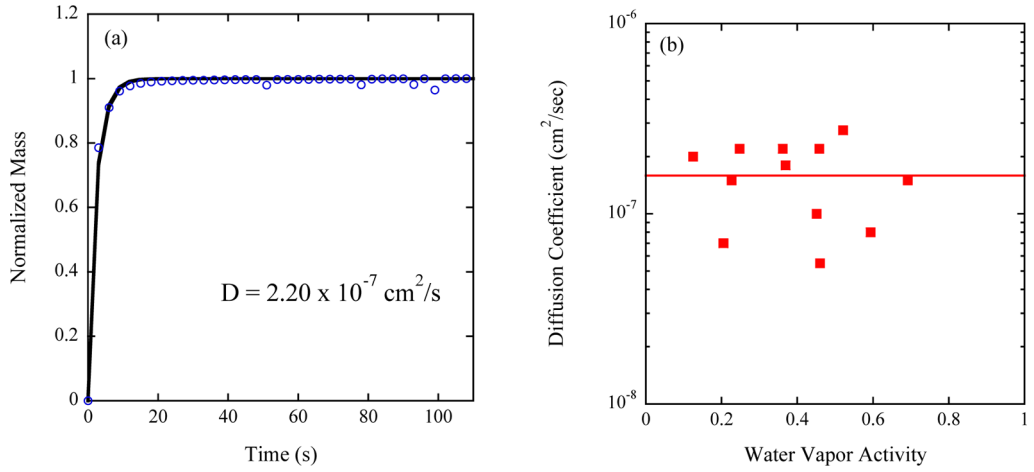

Figure 9. QCM data (a) water sorption kinetics in PLA at 35 °C in response to an external differential water vapor activity step change of 0.25 to 0.36. The solid black line represents a regression of the experimental data (open blue circles) to the solution to Fick's Second Law (eq 4), where the diffusion coefficient, D, was the only adjustable parameter. (b) Water vapor diffusion coefficients in PLA over a wide range of water activities at 35 °C.

experiments were examined. However, no changes in the infrared bands associated with the polymer could be quantified with confidence (i.e., low signal-to-noise ratio). We attribute this to a lower concentration of water in PLA when exposed to a vapor opposed to a liquid. Therefore, the dilation of the polymer could not be accurately quantified with time-resolved FTIR-ATR spectroscopy. Attempts to measure polymer relaxation in the presence of water vapor with laser dilatometry (accuracy of 0.1%) were also explored.[13] However, the dilation of the polymer was also outside the sensitivity of this apparatus as well.

Therefore, the water sorption kinetics data for all three experimental techniques were analyzed using a two-stage diffusion-relaxation model similar to the approach of Berens and Hopfenberg[10] with their analysis of the diffusion of organic vapors (e.g., vinyl chloride monomer, acetone, methanol, *n*-hexane) in glassy polymers (*e.g.*, polyvinyl chloride, polystyrene). Others have also proposed diffusion-relaxation models for glassy polymers.[20,21] In the Berens and Hopfenberg model, the total mass of penetrant uptake in the polymer is divided into two parts, one for the Fickian process and the other for the relaxation process:

$$M_t = M_{t,F} + M_{t,R} \tag{10}$$

where M_t is the total mass uptake at time t and $M_{t,F}$ and $M_{t,R}$ are the contributions of the Fickian and relaxation processes, respectively, at time t. Therefore, the Fickian solution (e.g., eq 4) can be inserted in for $M_{t,F}$, while an equation that describes relaxation can be inserted into $M_{t,R}$. In the work of Berens and Hopfenberg,[10] they examined diffusion into polymer microspheres and therefore their diffusion–relaxation model was expressed as

$$M_t = M_{\infty,F}\left(1 - \frac{6}{\pi^2}\sum_{n=1}^{\infty}\frac{1}{n^2}\exp[-n^2 k_F t]\right) + \sum_i M_{\infty,i}\exp[1 - \exp(-k_i t)] \tag{11}$$

In eq 11, the first part describes the Fickian solution in spherical coordinates, while the second part describes a series of simple first-order expressions to describe relaxation. In their work, all of their sorption kinetics data were regressed to eq 11 with the series extended to two terms, and therefore this regression included six fitting parameters: $M_{\infty,F}$, k_F, $M_{\infty,1}$, k_1, $M_{\infty,2}$, and k_2. The first two fitting parameters describe the total mass uptake due to the Fickian contribution, $M_{\infty,F}$, and a parameter that is related to the Fickian diffusion coefficient, k_F ($= \pi^2 D/4L^2$). The remaining four fitting parameters are the mass uptake and relaxation time constants due to the relaxation contribution.

In this work, we propose to minimize the number of fitting parameters by considering a single-relaxation process in the regression of the QSM, QCM, and FTIR-ATR sorption kinetics data. For the gravimetric experiments (QSM, QCM), a diffusion–relaxation model can thus be described as

$$M_t = M_{\infty,F}\left(1 - \sum_{n=0}^{\infty}\frac{8}{(2n+1)^2\pi^2}\times\exp\left[\frac{-D(2n+1)^2\pi^2 t}{4L^2}\right]\right) + M_{\infty,R}\times\exp[1 - \exp(-k_R t)] \tag{12}$$

where the first part describes the Fickian solution in Cartesian coordinates (eq 4) and the second part describes a first-order relaxation. In eq 12, four fitting parameters are evident, $M_{\infty,F}$, D, $M_{\infty,R}$, and k_R, where $M_{\infty,F}$ and D are the mass gain and diffusion coefficient attributed to the first Fickian stage, while $M_{\infty,R}$ and k_R are the mass gain and relaxation time constant from the second relaxation stage. To minimize the number of fitting parameters even further, a regression of the early time data to the Fickian solution (eq 4) can be performed (see Figures 7a and 9a), where the diffusion coefficient, D, is the only adjustable parameter and $M_{\infty,F}$ is known as the pseudoequilibrium sorption (dashed lines in Figure 2b,c). These values can be used to regress the sorption kinetics data over the entire experimental time scale to eq 12 with only two fitting parameters, $M_{\infty,R}$ and k_R. An example of this approach is shown in the regression of the QSM and QCM data in Figure 10a and 10b, where the insets show a regression of the early time data to the Fickian solution (eq 4) and the entire data set is regressed to the diffusion–relaxation model (eq 12). Figure 10 panels a and b show an adequate regression of the diffusion–relaxation model and the regression results for all QSM and QCM experiments ($M_{\infty,F}$, D, $M_{\infty,R}$, and k_R) are listed in Supporting Information, Table S4.

Similarly, the FTIR-ATR data can be regressed to a diffusion–relaxation model described as

dx.doi.org/10.1021/ie302342m | *Ind. Eng. Chem. Res.* 2013, 52, 8664–8673

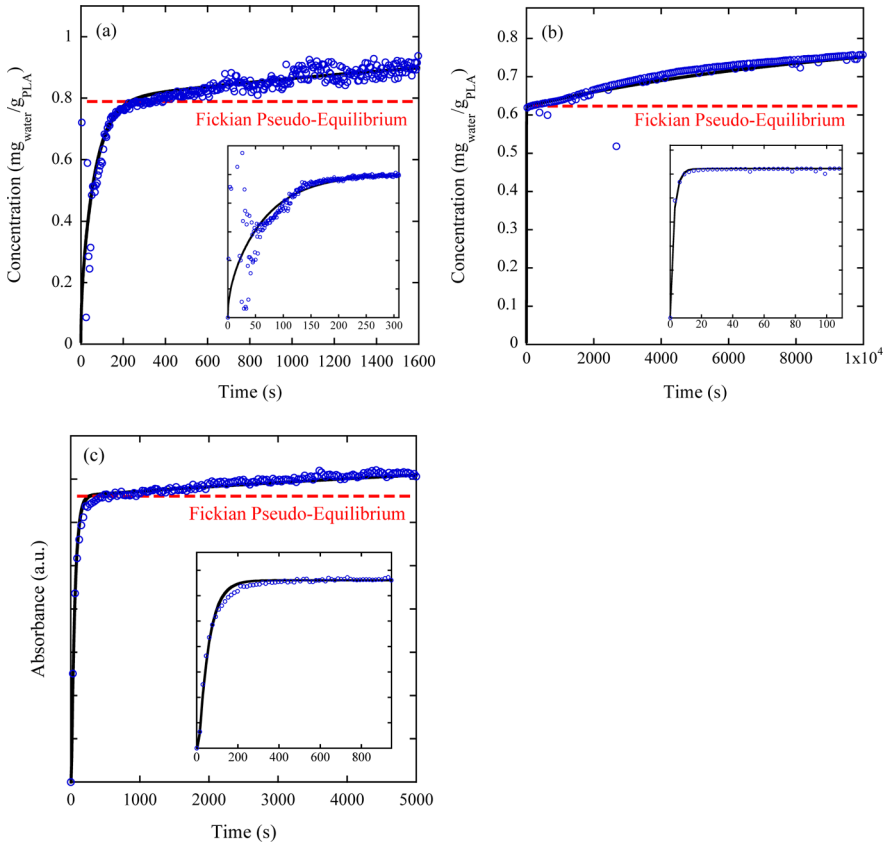

Figure 10. Results from regression to diffusion−relaxation model for (a) QSM ($M_{\infty,R}$ = 0.26 mg_{water}/g_{PLA} and $k_R = 3.4 \times 10^{-4}$ 1/s), and (b) QCM ($M_{\infty,R}$ = 0.20 mg_{water}/g_{PLA} and $k_R = 1.0 \times 10^{-4}$ 1/s), and (c) time-resolved FTIR-ATR spectroscopy ($A_{\infty,R} = 1.6 \times 10^{-3}$ au and $k_R = 7.9 \times 10^{-5}$ 1/s) in response to an external differential change in water vapor activity of 0.53 to 0.65, 0.25 to 0.36, and 0.54 to 0.75, respectively. The solid lines correspond to a regression to the diffusion−relaxation model (eqs 12, 12, and 13 for panels a, b, and c, respectively). The insets correspond to a magnified view of the early time data, where the solid lines correspond to a regression to the solution to Fick's Second Law (eqs 4, 4, and 9 for panels a, b, and c, respectively), where the diffusion coefficient, D, was the only adjustable parameter. The dashed lines correspond to Fickian pseudoequilibrium values.

$$A_t = A_{\infty,F}\left(1 - \frac{4}{\pi}\sum_{n=0}^{\infty}\frac{(-1)^n}{2n+1^2}\exp\left[\frac{-D(2n+1)^2\pi^2 t}{4L^2}\right]\right) + A_{\infty,R}\exp[1 - \exp(-k_R t)] \quad (13)$$

where the first part describes the FTIR-ATR Fickian solution in Cartesian coordinates (eq 9) and the second part describes a first-order relaxation. A similar regression method was used for FTIR-ATR data as described for QSM and QCM data. The early time data were regressed to the FTIR-ATR Fickian solution (eq 9) (similar to Figure 5a) to determine the diffusion coefficient, D, as the only adjustable parameter and a known $A_{\infty,F}$ from the pseudoequilibrium sorption (dashed line in Figures 2a). These values were used to regress the FTIR-ATR data over the entire experimental time scale to eq 13 with only two fitting parameters, $A_{\infty,R}$ and k_R. An example of this approach is shown in the regression of the FTIR-ATR data in Figure 10c, where the insets show a regression of the early time data to the FTIR-ATR Fickian solution (eq 9) and the entire data set is regressed to the diffusion−relaxation model (eq 13). Figure 10c shows an adequate regression of the entire data set to the diffusion−relaxation model, where the regression results of all FTIR-ATR experiments ($A_{\infty,F}$, D, $A_{\infty,R}$, and k_R) are listed in Supporting Information, Table S4.

A comparison of the diffusion coefficients, D ($= k_F 4L^2/\pi^2$) and relaxation time constants, k_R, in Supporting Information, Table S4, provides insights in the two-stage diffusion−relaxation phenomena. Berens and Hopfenberg[10] suggest that when $k_F \gg k_R$ then one should observe a rapid Fickian first stage followed by a slower discernible separate second relaxation-controlled sorption stage, while for $k_F \approx k_R$ the two stages would not be clearly separable. Supporting Information, Table S5 summarizes the results from Table S4, where the diffusion time ($\tau_F \approx L^2/D \approx \pi^2/k_F 4$) and relaxation time ($\tau_R \approx 1/k_R$) have been calculated from the regressed diffusion coefficients and relaxation time constants, respectively. Table S5 also reports a ratio of these times, which is referred to as the diffusion Deborah (De) number, where a high De corresponds to $k_F \gg k_R$ and a low De (approaching the value of 1) corresponds to $k_F \approx k_R$. In Table S5, the average De for FTIR-ATR, QSM, and QCM are on the order of 450, 40, and 3700, respectively. These high De values in all three experimental techniques corroborate with the observed separable and distinguishable two-stage diffusion-relaxation phenomena observed.

CONCLUSIONS

Data from three separate experimental techniques, QSM, QCM, and time-resolved FTIR-ATR spectroscopy all showed non-Fickian diffusion of water vapor in PLA. Specifically, this non-Fickian behavior was a result of the nonequilibrium state of the glassy polymer, where two-stage sorption kinetics was observed. These stages were distinctively separate over time, where Fickian behavior was observed at early times and polymer relaxation was observed at later times, indicated by a continuous, gradual uptake of water. Furthermore, a diffusion−relaxation model confirms the observed two-stage behavior, where high Deborah numbers

dx.doi.org/10.1021/ie302342m | Ind. Eng. Chem. Res. 2013, 52, 8664−8673

(relaxation time/diffusion time) were calculated. Calculated diffusion coefficients from all three experimental techniques were similar at all temperatures and activities studied, while relaxation time constants differed. The variation in the relaxation time constants may be a product of the different constraints on the polymer film for the different experimental techniques.

■ ASSOCIATED CONTENT

Supporting Information

Tabulated results from regression analysis of Fickian and diffusion−relaxation models are included. This material is available free of charge via the Internet at http://pubs.acs.org.

■ AUTHOR INFORMATION

Corresponding Author

*E-mail: elabd@drexel.edu.

Notes

The authors declare no competing financial interest.

■ ACKNOWLEDGMENTS

The authors acknowledge the financial support of the National Science Foundation (CAREER 0644593) and the United States Department of Agriculture and the United States Department of Energy (06GO96002). We, the authors of this manuscript, gratefully acknowledge Professor Giulio Sarti, not only for his outstanding contributions to science and engineering, but also for his significant impact on us and our work over the years. Professor Sarti has been a generous and insightful mentor to us all and we are forever indebted to him. Professor Elabd is also grateful to Professor Sarti for his generosity in hosting several of Dr. Elabd's PhD students in his laboratory over the years, e.g., Eric Davis, an author on this manuscript. We are all happy to be able to contribute this article for this special issue honoring Professor Sarti.

■ REFERENCES

(1) Auras, R.; Harte, B.; Selke, S. An Overview of Polylactides as Packaging Materials. *Macromol. Biosci.* **2004**, *4*, 835−864.

(2) Sinclair, R. G. The Case for Polylactic Acid as a Commodity Packaging Plastic. *J. Macromol. Sci., Part A: Pure Appl. Chem.* **1996**, *5*, 585−597.

(3) Williams, C. K.; Hillmyer, M. A. Polymers from Renewable Resources: A Perspective for a Special Issue of Polymer Reviews. *Polym. Rev.* **2008**, *48*, 1−10.

(4) Oliveira, N. S.; Gonçalves, C. M.; Coutinho, J. A. P.; Ferreira, A.; Dorgan, J.; Marrucho, I. M. Carbon Dioxide, Ethylene and Water Vapor Sorption in Poly(lactic acid). *Fluid Phase Equilib.* **2006**, *250*, 116−124.

(5) Siparsky, G. L.; Voorhees, K. J.; Dorgan, J. R.; Schilling, K. Water Transport in Polylactic Acid (PLA), PLA/Polycaprolactone Copolymers, and PLA/Polyethylene Glycol Blends. *J. Environ. Polym. Degradation* **1997**, *5*, 125−136.

(6) Drieskens, M.; Peeters, R.; Mullens, J.; Franco, D.; Lemstra, P. J.; Hristova-Bogaerds, D. G. Structure versus Properties Relationship of Poly(lactic acid). I. Effect of Crystallinity on Barrier Properties. *J. Polym. Sci., Part B: Polym. Phys.* **2009**, *47*, 2247−2258.

(7) Sharp, J. S.; Forrest, J. A.; Jones, R. A. L. Swelling of Poly(DL-lactide) and Polylactide-*co*-glycolide in Humid Environments. *Macromolecules* **2001**, *34*, 8752−8760.

(8) Davis, E. M.; Theryo, G.; Hillmyer, M. A.; Cairncross, R. A.; Elabd, Y. A. Liquid Water Transport in Polylactide Homo and Graft Copolymers. *ACS Appl. Mater. Interfaces* **2011**, *3*, 3997−4006.

(9) Cairncross, R. A.; Ramaswamy, S.; O'Connor, R. Moisture Sorption and Transport in Polylactide. *Int. Polym. Process.* **2007**, *22*, 33−37.

(10) Berens, A. R.; Hopfenberg, H. B. Diffusion and Relaxation in Glassy Polymer Powder: 2. Separation of Diffusion and Relaxation Parameters. *Polymer* **1978**, *19*, 489−496.

(11) Frish, H. L. Sorption and Transport in Glassy Polymers: A Review. *Polym. Eng. Sci.* **1980**, *20*, 2−13.

(12) Vrentas, J. S.; Jarzebski, C. M.; Duda, J. L. A Deborah Number for Diffusion in Polymer−Solvent Systems. *AIChE J.* **1975**, *21*, 894−901.

(13) Davis, E. M.; Minelli, M.; Giacinti Baschetti, M.; Sarti, G. C.; Elabd, Y. A. Non-equilibrium Sorption of Water in Polylactide. *Macromolecules* **2012**, *45*, 7486−7494.

(14) Crank, J. *Mathematics of Diffusion*, 2nd ed.; Wiley: New York, 2003.

(15) Vogt, B. D.; Lin, E. K.; Wu, W.; White, C. C. Effect of Film Thickness on the Validity of the Sauerbrey Equation for Hydrated Polyelectrolyte Films. *J. Phys. Chem. B* **2004**, *108*, 12685−12690.

(16) Yamamoto, Y.; Ferrari, M. C.; Giacinti Baschetti, M.; De Angelis, M. G.; Sarti, G. C. A Quartz Crystal Microbalance Study of Water Vapor Sorption in a Short Side-Chain PFSI Membrane. *Desalination* **2006**, *200*, 636−638.

(17) Elabd, Y. A.; Giacinti Baschetti, M.; Barbari, T. A. Time-Resolved FTIR-ATR Spectroscopy for the Measurement of Molecular Diffusion in Polymers. *J. Polym. Sci., Part B: Polym. Phys.* **2003**, *41*, 2794−2807.

(18) Elabd, Y. A. Diffusion in Polymers: Penetrant−Polymer and Penetrant−Penetrant Interactions. Ph.D. Dissertation, Johns Hopkins University; Baltimore, MD, 2000.

(19) Hallinan, D. T., Jr.; Elabd, Y. A. Diffusion of Water in Nafion Using Time-Resolved FTIR-ATR Spectroscopy. *J. Phys. Chem. B* **2009**, *113*, 4257−4266.

(20) Carlà, V.; Hussain, Y.; Grant, C.; Sarti, G. C.; Carbonell, R. G.; Doghieri, F. Modeling Sorption Kinetics of Carbon Dioxide in Glassy Polymeric Films Using the Nonequilibrium Thermodynamics Approach. *Ind. Eng. Chem. Res.* **2009**, *48*, 3844−3854.

(21) Dimos, V.; Sanopoulou, M. Determination of Sorption Kinetic Parameters Using the Relaxation-Dependent Solubility Model in the Methanol Vapor-Poly(methyl methacrylate) System. *J. Appl. Polym. Sci.* **2006**, *100*, 2278−2288.